
Optimization Methods for Sparse Pseudo-Likelihood Graphical Model Selection

Sang-Yun Oh
 Computational Research Division
 Lawrence Berkeley National Lab
 syoh@lbl.gov

Onkar Dalal
 Stanford University
 onkar@alumni.stanford.edu

Kshitij Khare
 Department of Statistics
 University of Florida
 kdkhare@stat.ufl.edu

Bala Rajaratnam
 Department of Statistics
 Stanford University
 brajarat@stanford.edu

Abstract

Sparse high dimensional graphical model selection is a popular topic in contemporary machine learning. To this end, various useful approaches have been proposed in the context of ℓ_1 -penalized estimation in the Gaussian framework. Though many of these inverse covariance estimation approaches are demonstrably scalable and have leveraged recent advances in convex optimization, they still depend on the Gaussian functional form. To address this gap, a convex pseudo-likelihood based partial correlation graph estimation method (CONCORD) has been recently proposed. This method uses coordinate-wise minimization of a regression based pseudo-likelihood, and has been shown to have robust model selection properties in comparison with the Gaussian approach. In direct contrast to the parallel work in the Gaussian setting however, this new convex pseudo-likelihood framework has not leveraged the extensive array of methods that have been proposed in the machine learning literature for convex optimization. In this paper, we address this crucial gap by proposing two proximal gradient methods (CONCORD-ISTA and CONCORD-FISTA) for performing ℓ_1 -regularized inverse covariance matrix estimation in the pseudo-likelihood framework. We present timing comparisons with coordinate-wise minimization and demonstrate that our approach yields tremendous payoffs for ℓ_1 -penalized partial correlation graph estimation outside the Gaussian setting, thus yielding the fastest and most scalable approach for such problems. We undertake a theoretical analysis of our approach and rigorously demonstrate convergence, and also derive rates thereof.

1 Introduction

1.1 Background

Sparse inverse covariance estimation has received tremendous attention in the machine learning, statistics and optimization communities. These sparse models, popularly known as graphical models, have widespread use in various applications, especially in high dimensional settings. The most popular inverse covariance estimation framework is arguably the ℓ_1 -penalized Gaussian likelihood optimization framework as given by

$$\underset{\Omega \in \mathbf{S}_{++}^p}{\text{minimize}} \quad -\log \det \Omega + \text{tr}(S\Omega) + \lambda \|\Omega\|_1$$

where \mathbf{S}_{++}^p denotes the space of p -dimensional positive definite matrices, and ℓ_1 -penalty is imposed on the elements of $\Omega = (\omega_{ij})_{1 \leq i, j \leq p}$ by the term $\|\Omega\|_1 = \sum_{i, j} |\omega_{ij}|$ along with the scaling factor $\lambda > 0$. The matrix S denotes the

sample covariance matrix of the data $\mathbf{Y} \in \mathbb{R}^{n \times p}$. As the ℓ_1 -penalized log likelihood is convex, the problem becomes more tractable and has benefited from advances in convex optimization. Recent efforts in the literature on Gaussian graphical models therefore have focused on developing principled methods which are increasingly more and more scalable. The literature on this topic is simply enormous and for the sake of brevity, space constraints and the topic of this paper, we avoid an extensive literature review by referring to the references in the seminal work of Banerjee et al. [2008] and the very recent work of Dalal and Rajaratnam [2014]. These two papers contain references to recent work, including past NIPS conference proceedings.

1.2 The CONCORD method

Despite their tremendous contributions, one shortcoming of the traditional approaches to ℓ_1 -penalized likelihood maximization is the restriction to the Gaussian assumption. To address this gap, a number of ℓ_1 -penalized pseudo-likelihood approaches have been proposed: SPACE Peng et al. [2009] and SPLICE Rocha et al. [2008], SYMLASSO Friedman et al. [2010]. These approaches are either not convex, and/or convergence of corresponding maximization algorithms are not established. In this sense, non-Gaussian partial correlation graph estimation methods have lagged severely behind, despite the tremendous need to move beyond the Gaussian framework for obvious practical reasons. In very recent work, a convex pseudo-likelihood approach with good model selection properties called CONCORD Khare et al. [2014] was proposed. The CONCORD algorithm minimizes

$$Q_{\text{con}}(\Omega) = -\sum_{i=1}^p n \log \omega_{ii} + \frac{1}{2} \sum_{i=1}^p \|\omega_{ii} \mathbf{Y}_i + \sum_{j \neq i} \omega_{ij} \mathbf{Y}_j\|_2^2 + n\lambda \sum_{1 \leq i < j \leq p} |\omega_{ij}| \quad (1)$$

via cyclic coordinate-wise descent that alternates between updating off-diagonal elements and diagonal elements. It is straightforward to show that operators T_{ij} for updating $(\omega_{ij})_{1 \leq i < j \leq p}$ (holding $(\omega_{ii})_{1 \leq i \leq p}$ constant) and T_{ii} for updating $(\omega_{ii})_{1 \leq i \leq p}$ (holding $(\omega_{ij})_{1 \leq i < j \leq p}$ constant) are given by

$$(T_{ij}(\Omega))_{ij} = \frac{S_\lambda \left(- \left(\sum_{j' \neq j} \omega_{ij'} s_{jj'} + \sum_{i' \neq i} \omega_{i'j} s_{ii'} \right) \right)}{s_{ii} + s_{jj}} \quad (2)$$

$$(T_{ii}(\Omega))_{ii} = \frac{-\sum_{j \neq i} \omega_{ij} s_{ij} + \sqrt{\left(\sum_{j \neq i} \omega_{ij} s_{ij} \right)^2 + 4s_{ii}}}{2s_{ii}}. \quad (3)$$

This coordinate-wise algorithm is shown to converge to a global minima though no rate is given [Khare et al., 2014]. Note that the equivalent problem assuming a Gaussian likelihood has seen much development in the last ten years, but a parallel development for the recently introduced CONCORD framework is lacking for obvious reasons. We address this important gap by proposing state-of-the-art proximal gradient techniques to minimize Q_{con} . A rigorous theoretical analysis of the pseudo-likelihood framework and the associated proximal gradient methods which are proposed is undertaken. We establish rates of convergence and also demonstrate that our approach can lead to massive computational speed-ups, thus yielding extremely fast and principled solvers for the sparse inverse covariance estimation problem outside the Gaussian setting.

2 CONCORD using proximal gradient methods

The penalized matrix version the CONCORD objective function in (1) is given by

$$Q_{\text{con}}(\Omega) = \frac{n}{2} \left[-\log |\Omega_D^2| + \text{tr}(\mathbf{S}\Omega^2) + \lambda \|\Omega_X\|_1 \right]. \quad (4)$$

where Ω_D and Ω_X denote the diagonal and off-diagonal elements of Ω . We will use the notation $A = A_D + A_X$ to split any matrix A into its diagonal and off-diagonal terms.

This section proposes a scalable and thorough approach to solving the CONCORD objective function using recent advances in convex optimization and derives rates of convergence for such algorithms. In particular, we use proximal gradient-based methods to achieve this goal and demonstrate the efficacy of such methods for the non-Gaussian graphical modeling problem. First, we propose CONCORD-ISTA and CONCORD-FISTA in section 2.1: methods which are inspired by the iterative soft-thresholding algorithms in Beck and Teboulle [2009]. We undertake a comprehensive treatment of the CONCORD optimization problem by also investigating the dual of the CONCORD problem. Other popular methods in the literature, including the potential use of alternating minimization algorithm and the second order proximal Newtons method CONCORD-PNOPT, are considered in Supplemental section A.5.

Algorithm 1 CONCORD-ISTA

Input: sample covariance matrix S , penalty matrix Λ Initialize: $\Omega^{(0)} \in \mathbb{S}_+^p$, $\tau_{(0,0)} \leq 1$, $c < 1$, $\Delta_{\text{subg}} = 2\epsilon_{\text{subg}}$.**while** $\Delta_{\text{subg}} > \epsilon_{\text{subg}}$ **or** $\Delta_{\text{func}} > \epsilon_{\text{func}}$ **do** Compute ∇h_1 :

$$G^{(k)} = -\left(\Omega_D^{(k)}\right)^{-1} + \frac{1}{2}(S\Omega^{(k)} + \Omega^{(k)}S)$$

 Compute τ_k : Largest $\tau_k \in \{c^j \tau_{(k,0)}\}_{j=0,1,\dots}$ such that,

$$\Omega^{(k+1)} = \mathcal{S}_{\tau_k \Lambda} \left(\Omega^{(k)} - \tau_k G^{(k)} \right) \text{ satisfies (8).}$$

 Update: $\Omega^{(k+1)}$ using the appropriate step size. Compute next initial step size: $\tau_{(k+1,0)}$

Compute convergence criteria:

$$\Delta_{\text{subg}} = \frac{\|\nabla h_1(\Omega^{(k)}) + \partial h_2(\Omega^{(k)})\|}{\|\Omega^{(k)}\|}.$$

end while

Algorithm 2 CONCORD-FISTA

Input: sample covariance matrix S , penalty matrix Λ Initialize: $(\Theta^{(1)} =)\Omega^{(0)} \in \mathbb{S}_+^p$, $\alpha_1 = 1$, $\tau_{(0,0)} \leq 1$, $c < 1$, $\Delta_{\text{subg}} = 2\epsilon_{\text{subg}}$.**while** $\Delta_{\text{subg}} > \epsilon_{\text{subg}}$ **or** $\Delta_{\text{func}} > \epsilon_{\text{func}}$ **do** Compute ∇h_1 :

$$G^{(k)} = -\left(\Theta_D^{(k)}\right)^{-1} + \frac{1}{2}(S\Theta^{(k)} + \Theta^{(k)}S)$$

 Compute τ_k : Largest $\tau_k \in \{c^j \tau_{(k,0)}\}_{j=0,1,\dots}$ such that,

$$\Omega^{(k)} = \mathcal{S}_{\tau_k \Lambda} \left(\Theta^{(k)} - \tau_k G^{(k)} \right) \text{ satisfies (8)}$$

 Update: $\alpha_{k+1} = (1 + \sqrt{1 + 4\alpha_k^2})/2$

$$\text{Update: } \Theta^{(k+1)} = \Omega^{(k)} + \left(\frac{\alpha_k - 1}{\alpha_{k+1}}\right) (\Omega^{(k)} - \Omega^{(k-1)})$$

 Compute next initial step size: $\tau_{(k+1,0)}$

Compute convergence criteria:

$$\Delta_{\text{subg}} = \frac{\|\nabla h_1(\Omega^{(k)}) + \partial h_2(\Omega^{(k)})\|}{\|\Omega^{(k)}\|}.$$

end while

2.1 Iterative Soft Thresholding Algorithms: CONCORD-ISTA, CONCORD-FISTA

The iterative soft-thresholding algorithms (ISTA) have recently gained popularity after the seminal paper by Beck and Teboulle [2009]. The ISTA methods are based on the Forward-Backward Splitting method from Rockafellar [1976] and Nesterov's accelerated gradient methods Nesterov [1983] using soft-thresholding as the proximal operator for the ℓ_1 -norm. The essence of the proximal gradient algorithms is to divide the objective function into a smooth part and a non-smooth part, then take a proximal step (w.r.t. the non-smooth part) in the negative gradient direction of the smooth part. Nesterov's accelerated gradient extension Nesterov [1983] uses a combination of gradient and momentum steps to achieve accelerated rates of convergence. In this section, we apply these methods in the context of CONCORD which also has a composite objective function.

The matrix CONCORD objective function (4) can be split into a smooth part $h_1(\Omega)$ and a non-smooth part $h_2(\Omega)$:

$$h_1(\Omega) = -\log \det \Omega_D + \frac{1}{2} \text{tr}(\Omega S \Omega), \quad h_2(\Omega) = \lambda \|\Omega_X\|_1. \quad (5)$$

The gradient and hessian of the smooth function h_1 are given by

$$\begin{aligned} \nabla h_1(\Omega) &= \Omega_D^{-1} + \frac{1}{2}(S\Omega^T + \Omega S), \\ \nabla^2 h_1(\Omega) &= \sum_{i=1}^{i=p} \omega_{ii}^{-2} [e_i e_i^T \otimes e_i e_i^T] + \frac{1}{2}(S \otimes I + I \otimes S), \end{aligned} \quad (6)$$

where e_i is a column vector of zeros except for a one in the i -th position. The proximal operator for the non-smooth function h_2 is given by element-wise soft-thresholding operator \mathcal{S}_λ as

$$\begin{aligned} \text{prox}_{h_2}(\Omega) &= \arg \min_{\Theta} \left\{ h_2(\Theta) + \frac{1}{2} \|\Omega - \Theta\|_F^2 \right\} \\ &= \mathcal{S}_\Lambda(\Omega) = \text{sign}(\Omega) \max\{|\Omega| - \Lambda, 0\}, \end{aligned} \quad (7)$$

where Λ is a matrix with 0 diagonal and λ for each off-diagonal entry. The details of the proximal gradient algorithm CONCORD-ISTA are given in Algorithm 1, and the details of the accelerated proximal gradient algorithm CONCORD-FISTA are given in Algorithm 2.

2.2 Choice of step size

In the absence of a good estimate of the Lipschitz constant L , the step size for each iteration of CONCORD-ISTA and CONCORD-FISTA is chosen using backtracking line search. The line search for iteration k starts with an initial step size $\tau_{(k,0)}$ and reduces the step with a constant factor c until the new iterate satisfies the sufficient descent condition:

$$h_1(\Omega^{(k+1)}) \leq \mathcal{Q}(\Omega^{(k+1)}, \Omega^{(k)}) \quad (8)$$

where,

$$\mathcal{Q}(\Omega, \Theta) = h_1(\Theta) + \text{tr}((\Omega - \Theta)^T \nabla h_1(\Theta)) + \frac{1}{2\tau} \|\Omega - \Theta\|_F^2.$$

In section 4, we have implemented algorithms choosing the initial step size in three different ways: (a) a constant starting step size ($=1$), (b) the feasible step size from the previous iteration τ_{k-1} , (c) the step size heuristic of Barzilai-Borwein. The Barzilai-Borwein heuristic step size is given by

$$\tau_{k+1,0} = \frac{\text{tr}((\Omega^{(k+1)} - \Omega^{(k)})^T (\Omega^{(k+1)} - \Omega^{(k)}))}{\text{tr}((\Omega^{(k+1)} - \Omega^{(k)})^T (G^{(k+1)} - G^{(k)}))}. \quad (9)$$

This is an approximation of the secant equation which works as a proxy for second order information using successive gradients (see Barzilai and Borwein [1988] for details).

2.3 Computational complexity

After the one time calculation of S , the most significant computation for each iteration in CONCORD-ISTA and CONCORD-FISTA algorithms is the matrix-matrix multiplication $W = S\Omega$ in the gradient term. If s is the number of non-zeros in Ω , then W can be computed using $\mathcal{O}(sp^2)$ operations if we exploit the extreme sparsity in Ω . The second matrix-matrix multiplication for the term $\text{tr}(\Omega(S\Omega))$ can be computed efficiently using $\text{tr}(\Omega W) = \sum \omega_{ij} w_{ij}$ over the set of non-zero ω_{ij} 's. This computation only requires $\mathcal{O}(s)$ operations. The remaining computations are all at the element level which can be completed in $\mathcal{O}(p^2)$ operations. Therefore, the overall computational complexity for each iteration reduces to $\mathcal{O}(sp^2)$. On the other hand, the proximal gradient algorithms for the Gaussian framework require inversion of a full $p \times p$ matrix which is non-parallelizable and requires $\mathcal{O}(p^3)$ operations. The coordinate-wise method for optimizing CONCORD in Khare et al. [2014] also requires cycling through the p^2 entries of Ω in specified order and thus does not allow parallelization. In contrast, CONCORD-ISTA and CONCORD-FISTA can use 'perfectly parallel' implementations to distribute the above matrix-matrix multiplications. At no step do we need to keep all of the dense matrices $S, S\Omega, \nabla h_1$ on a single machine. Therefore, CONCORD-ISTA and CONCORD-FISTA are scalable to any high dimensions restricted only by the number of machines.

3 Convergence Analysis

In this section, we prove convergence of CONCORD-ISTA and CONCORD-FISTA methods along with their respective convergence rates of $\mathcal{O}(1/k)$ and $\mathcal{O}(1/k^2)$. We would like to point out that, although the authors in Khare et al. [2014] provide a proof of convergence for their coordinate-wise minimization algorithm for CONCORD, they do not provide any rates of convergence. The arguments for convergence leverage the results in Beck and Teboulle [2009] but require some essential ingredients. We begin with proving lower and upper bounds on the diagonal entries ω_{kk} for Ω belonging to a level set of $Q_{\text{con}}(\Omega)$. The lower bound on the diagonal entries of Ω establishes Lipschitz continuity of the gradient $\nabla h_1(\Omega)$ based on the hessian of the smooth function as stated in (6). The proof for the lower bound uses the existence of an upper bound on the diagonal entries. Hence, we prove both bounds on the diagonal entries. We begin by defining a level set \mathcal{C}_0 of the objective function starting with an arbitrary initial point $\Omega^{(0)}$ with a finite function value as

$$\mathcal{C}_0 = \left\{ \Omega \mid Q_{\text{con}}(\Omega) \leq Q_{\text{con}}(\Omega^{(0)}) = M \right\}. \quad (10)$$

For the positive semidefinite matrix S , let U denote $\frac{1}{\sqrt{2}}$ times the upper triangular matrix from the LU decomposition of S , such that $S = 2U^T U$ (the factor 2 simplifies further arithmetic). Assuming the diagonal entries of S to be strictly nonzero (if $s_{kk} = 0$, then the k^{th} component can be ignored upfront since it has zero variance and is equal to a constant for every data point), we have at least one k such that $u_{ki} \neq 0$ for every i . Using this, we prove the following theorem bounding the diagonal entries of Ω .

Theorem 3.1. For any symmetric matrix Ω satisfying $\Omega \in \mathcal{C}_0$, the diagonal elements of Ω are bounded above and below by constants which depend only on M , λ and S . In other words,

$$0 < a_{M,\lambda,S} \leq |\omega_{kk}| \leq b_{M,\lambda,S}, \quad \forall k = 1, 2, \dots, p,$$

for some constants $a_{M,\lambda,S}$ and $b_{M,\lambda,S}$.

Proof. (a) Upper bound: Suppose $|\omega_{ii}| = \max\{|\omega_{kk}|, \text{ for } k = 1, 2, \dots, p\}$. Then, we have

$$\begin{aligned} M &= Q_{\text{con}}(\Omega^{(0)}) \geq Q_{\text{con}}(\Omega) = h_1(\Omega) + h_2(\Omega) \\ &\geq -\log \det \Omega_D + \text{tr}((U\Omega)^T(U\Omega)) + \lambda \|\Omega_X\|_1 \\ &= -\log \det \Omega_D + \|U\Omega\|_F^2 + \lambda \|\Omega_X\|_1. \end{aligned} \quad (11)$$

Considering only the ki^{th} entry in the Frobenious norm term and the i^{th} column penalty in the third term we get

$$M \geq -p \log |\omega_{ii}| + \left(\sum_{j=k}^{j=p} u_{kj} \omega_{ji} \right)^2 + \lambda \sum_{j=k, j \neq i}^{j=p} |\omega_{ji}|. \quad (12)$$

Now, suppose $|u_{ki} \omega_{ii}| = z$ and $\sum_{j=k, j \neq i}^{j=p} u_{kj} \omega_{ji} = x$. Then

$$|x| \leq \sum_{j=k, j \neq i}^{j=p} |u_{kj}| |\omega_{ji}| \leq \bar{u} \sum_{j=k, j \neq i}^{j=p} |\omega_{ji}|,$$

where $\bar{u} = \max\{|u_{kj}|, \text{ for } j = k, k+1, \dots, p \text{ and } j \neq i\}$. Going back to the inequality (12), for $\bar{\lambda} = \frac{\lambda}{2\bar{u}}$, we have

$$\bar{M} = M + \bar{\lambda}^2 - p \log |u_{ki}| \geq -p \log z + (z+x)^2 + 2\bar{\lambda}|x| + \bar{\lambda}^2 \quad (13)$$

$$= -p \log z + (z+x + \bar{\lambda} \text{sign}(x))^2 - 2\bar{\lambda}z \text{sign}(x) \quad (14)$$

Here, if $x \geq 0$, then $\bar{M} \geq -p \log z + z^2$ using the first inequality (13), and if $x < 0$, then $\bar{M} \geq -p \log z + 2\bar{\lambda}z$ using the second inequality (14). In either cases, the functions $-p \log z + z^2$ and $-p \log z + 2\bar{\lambda}z$ are unbounded as $z \rightarrow \infty$. Hence, the upper bound of \bar{M} on these functions guarantee an upper bound $b_{M,\lambda,S}$ such that $|\omega_{ii}| \leq b_{M,\lambda,S}$. Therefore, $|\omega_{kk}| \leq b_{M,\lambda,S}$ for all $k = 1, 2, \dots, p$.

(b) Lower bound: By positivity of the trace term and the ℓ_1 term (for off-diagonals), we have

$$M \geq -\log \det \Omega_D = \sum_{i=1}^{i=p} -\log |\omega_{ii}|. \quad (15)$$

The negative log function $g(z) = -\log(z)$ is a convex function with a lower bound at $z^* = b_{M,\lambda,S}$ with $g(z^*) = -\log b_{M,\lambda,S}$. Therefore, for any $k = 1, 2, \dots, p$, we have

$$M \geq \sum_{i=1}^{i=p} -\log |\omega_{ii}| \geq -(p-1) \log b_{M,\lambda,S} - \log |\omega_{kk}|. \quad (16)$$

Simplifying the above equation, we get the lower bound $a_{M,\lambda,S}$ on the diagonal entries ω_{kk} . More specifically,

$$\log |\omega_{kk}| \geq -M - (p-1) \log b_{M,\lambda,S}.$$

Therefore, $|\omega_{kk}| \geq a_{M,\lambda,S} = e^{-M-(p-1)\log b_{M,\lambda,S}} > 0$ serves as a lower bound for all $k = 1, 2, \dots, p$. \square

Given that the function values are non-increasing along the iterates of Algorithms 1, 2 and 3, the sequence of $\Omega^{(k)}$ satisfy $\Omega^{(k)} \in \mathcal{C}_0$ for $k = 1, 2, \dots$. The lower bounds on the diagonal elements of $\Omega^{(k)}$ provides the Lipschitz continuity using

$$\nabla^2 h_1(\Omega^{(k)}) \preceq \left(a_{M,\lambda,S}^{-2} + \|S\|_2 \right) (I \otimes I). \quad (17)$$

Therefore, using the mean-value theorem, the gradient ∇h_1 satisfies

$$\|\nabla h_1(\Omega) - \nabla h_1(\Theta)\|_F \leq L \|\Omega - \Theta\|_F, \quad (18)$$

with the Lipschitz continuity constant $L = a_{M,\lambda,S}^{-2} + \|S\|_2$. The remaining argument for convergence follows from the theorems in Beck and Teboulle [2009].

Theorem 3.2. ([Beck and Teboulle, 2009, Theorem 3.1]). Let $\{\Omega^{(k)}\}$ be the sequence generated by either Algorithm 1 with constant step size or with backtracking line-search. Then for any $k \geq 1$,

$$Q_{con}(\Omega^{(k)}) - Q_{con}(\Omega^*) \leq \frac{\alpha L \|\Omega^{(0)} - \Omega^*\|_F^2}{2k} \quad (19)$$

for the solution Ω^* , where $\alpha = 1$ for the constant step size setting and $\alpha = c$ for the backtracking step size setting.

Theorem 3.3. ([Beck and Teboulle, 2009, Theorem 4.4]). For the sequences $\{\Omega^{(k)}\}, \{\Theta^{(k)}\}$ generated by Algorithm 2, for any $k \geq 1$,

$$Q_{con}(\Omega^{(k)}) - Q_{con}(\Omega^*) \leq \frac{2\alpha L \|\Omega^{(0)} - \Omega^*\|_F^2}{(k+1)^2} \quad (20)$$

for the solution Ω^* , where $\alpha = 1$ for the constant step size setting and $\alpha = c$ for the backtracking step size setting.

Hence, CONCORD-ISTA and CONCORD-FISTA converge at the rates of $\mathcal{O}(1/k)$ and $\mathcal{O}(1/k^2)$ for the k^{th} iteration.

4 Implementation & Numerical Experiments

In this section, we outline algorithm implementation details and present results of our comprehensive numerical evaluation. Section 4.1 gives performance comparisons from using synthetic multivariate Gaussian datasets. These datasets are generated from a wide range of sample sizes (n) and dimensionality (p). Additionally, convergence of CONCORD-ISTA and CONCORD-FISTA will be illustrated. Section 4.2 has timing results from analyzing a real breast cancer dataset with outliers. Comparisons are made to the coordinate-wise CONCORD implementation in `gconcord` package for R available at <http://cran.r-project.org/web/packages/gconcord/>.

For implementing the proposed algorithms, we can take advantage of existing linear algebra libraries. Most of the numerical computations in Algorithms 1 and 2 are linear algebra operations, and, unlike the sequential coordinate-wise CONCORD algorithm, CONCORD-ISTA and CONCORD-FISTA implementations can solve increasingly larger problems as more and more scalable and efficient linear algebra libraries are made available. For this work, we opted to use Eigen library [Guennebaud, Jacob, et al., 2010] for its sparse linear algebra routines written in C++. Algorithms 1 and 2 were also written in C++ then interfaced to R for testing. Table 1 gives names for various CONCORD-ISTA and CONCORD-FISTA versions using different initial step size choices.

4.1 Synthetic Datasets

Synthetic datasets were generated from true sparse positive random Ω matrices of three sizes: $p = \{1000, 3000, 5000\}$. Instances of random matrices used here consist of 4995, 14985 and 24975 non-zeros, corresponding to 1%, 0.33% and 0.20% edge densities, respectively. For each p , three random samples of sizes $n = \{0.25p, 0.75p, 1.25p\}$ were used as inputs. The initial guess, $\Omega^{(0)}$, and the convergence criteria was matched to those of coordinate-wise CONCORD implementation. Highlights of the results are summarized below, and the complete set of comparisons are given in Supplementary materials Section A.

For synthetic datasets, our experiments indicate that two variations of the CONCORD-ISTA method show little performance difference. However, `ccista_0` was marginally faster in our tests. On the other hand, `ccfista_1` variation of CONCORD-FISTA that uses $\tau_{(k+1,0)} = \tau_k$ as initial step size was significantly faster than `ccfista_0`. Table 2 gives actual running times for the two best performing algorithms, `ccista_0` and `ccfista_1`, against the coordinate-wise `concord`. As p and n increase `ccista_0` performs very well. For smaller n and λ , coordinate-wise `concord` performs well (more in Supplemental section A). This can be attributed to $\min(\mathcal{O}(np^2), \mathcal{O}(p^3))$ computational complexity of coordinate-wise CONCORD [Khare et al., 2014], and the sparse linear algebra routines used in CONCORD-ISTA and CONCORD-FISTA implementations slowing down as the number of non-zero elements in Ω increases. On the other hand, for large n fraction ($n = 1.25p$), the proposed methods `ccista_0` and `ccfista_1` are significantly faster than coordinate-wise `concord`. In particular, when $p = 5000$ and $n = 6250$, the speed-up of `ccista_0` can be as much as 150 times over coordinate-wise `concord`.

Convergence behavior of CONCORD-ISTA and CONCORD-FISTA methods is shown in Figure 1. The best performing algorithms `ccista_0` and `ccfista_1` are shown. The vertical axis is the subgradient Δ_{subg} (See Algorithms 1, 2). Plots show that `ccista_0` seems to converge at a constant rate much faster than `ccfista_1` that appears to slow

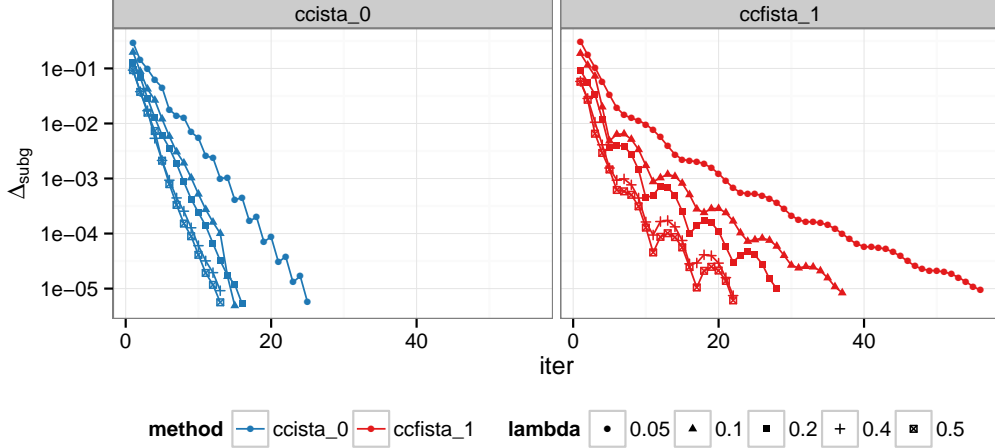


Figure 1: Convergence of CONCORD-ISTA and CONCORD-FISTA. Convergence threshold is $\Delta_{\text{subg}} < 10^{-5}$

down after a few initial iterations. While the theoretical convergence results from section 3 prove convergence rates of $\mathcal{O}(1/k)$ and $\mathcal{O}(1/k^2)$ for CONCORD-ISTA and CONCORD-FISTA, in practice, `ccista_0` with constant step size performed the fastest for the tests in this section.

4.2 Real Data

Real datasets arising from various physical and biological sciences often are not multivariate Gaussian and can have outliers. Hence, convergence characteristic may be different on such datasets. In this section, the performance of proposed methods are assessed on a breast cancer dataset [Chang et al., 2005]. This dataset contains expression levels of 24481 genes on 266 patients with breast cancer. Following the approach in Khare et al. [2014], the number of genes are reduced by utilizing clinical information that is provided together with the microarray expression dataset. In particular, survival analysis via univariate Cox regression with patient survival times is used to select a subset of genes closely associated with breast cancer. A choice of p-value < 0.03 yields a reduced dataset with $p = 4433$ genes.

Often times, graphical model selection algorithms are applied in a non-Gaussian and $n \ll p$ setting such as the case here. In this $n \ll p$ setting, coordinate-wise CONCORD algorithm is especially fast due to its computational complexity $\mathcal{O}(np^2)$. However, even in this setting, the newly proposed methods `ccista_0`, `ccista_1`, and `ccfista_1` perform competitively to, or often better than, `concord` as illustrated in Table 3. On this real dataset, `ccista_1` performed the fastest whereas `ccista_0` was the fastest on synthetic datasets.

5 Conclusion

The Gaussian graphical model estimation or inverse covariance estimation has seen tremendous advances in the past few years. In this paper we propose using proximal gradient methods to solve the general non-Gaussian sparse inverse covariance estimation problem. Rates of convergence were established for the CONCORD-ISTA and CONCORD-FISTA algorithms. Coordinate-wise minimization has been the standard approach to this problem thus far, and we provide numerical results comparing CONCORD-ISTA/FISTA and coordinate-wise minimization. We demonstrate that CONCORD-ISTA outperforms coordinate-wise in general, and in high dimensional settings CONCORD-ISTA can outperform coordinate-wise optimization by orders of magnitude. The methodology is also tested on real data sets. We undertake a comprehensive treatment of the problem by also examining the dual formulation and consider methods to maximize the dual objective. We note that efforts similar to ours for the Gaussian case has appeared in not one, but several NIPS and other publications. Our approach on the other hand gives a complete and thorough treatment of the non-Gaussian partial correlation graph estimation problem, all in this one self-contained paper.

Table 1: Naming convention for step size variations

Variation	Method	Initial step size
concord	CONCORD	-
ccista_0	CONCORD-ISTA	Constant
ccista_1	CONCORD-ISTA	Barzilai-Borwein
ccfista_0	CONCORD-FISTA	Constant
ccfista_1	CONCORD-FISTA	τ_k

Table 2: Timing comparison of concord and proposed methods: ccista_0 and ccfista_1.

p	n	λ	NZ%	concord		ccista_0		ccfista_1	
				iter	seconds	iter	seconds	iter	seconds
1000	250	0.150	1.52	9	3.2	13	1.8	20	3.3
		0.163	0.99	9	2.6	18	2.0	26	3.3
		0.300	0.05	9	2.6	15	1.2	23	2.7
	750	0.090	1.50	9	8.9	11	1.4	17	2.5
		0.103	0.76	9	8.4	15	1.6	24	3.3
		0.163	0.23	9	8.0	15	1.6	24	2.8
	1250	0.071	1.41	9	41.3	10	1.4	17	2.9
		0.077	0.97	9	40.5	15	1.7	24	3.3
		0.163	0.23	9	43.8	13	1.2	23	2.8
3000	750	0.090	1.10	17	147.4	20	32.4	25	53.2
		0.103	0.47	17	182.4	28	36.0	35	60.1
		0.163	0.08	16	160.1	28	28.3	26	39.9
	2250	0.053	1.07	16	388.3	17	28.5	17	39.6
		0.059	0.56	16	435.0	28	38.5	26	61.9
		0.090	0.16	16	379.4	16	19.9	15	23.6
	3750	0.040	1.28	16	2854.2	17	33.0	17	47.3
		0.053	0.28	16	2921.5	15	23.5	16	31.4
		0.163	0.07	15	2780.5	25	35.1	32	56.1
5000	1250	0.066	1.42	17	832.7	32	193.9	37	379.2
		0.077	0.53	17	674.7	30	121.4	35	265.8
		0.103	0.10	17	667.6	27	81.2	33	163.0
	3750	0.039	1.36	17	2102.8	18	113.0	17	176.3
		0.049	0.31	17	1826.6	16	73.4	17	107.4
		0.077	0.10	17	2094.7	29	95.8	33	178.1
	6250	0.039	0.27	17	15629.3	17	93.9	17	130.0
		0.077	0.10	17	15671.1	27	101.0	25	123.9
		0.163	0.04	16	14787.8	26	97.3	34	173.7

Table 3: Running time comparison on breast cancer dataset

λ	NZ%	concord		ccista_0		ccista_1		ccfista_0		ccfista_1	
		iter	sec	iter	sec	iter	sec	iter	sec	iter	sec
0.450	0.110	80	724.5	132	686.7	123	504.0	250	10870.3	201	672.6
0.451	0.109	80	664.2	129	669.2	112	457.0	216	7867.2	199	662.9
0.454	0.106	80	690.3	130	686.2	81	352.9	213	7704.2	198	677.8
0.462	0.101	79	671.6	125	640.4	109	447.1	214	7978.4	196	646.3
0.478	0.088	77	663.3	117	558.6	87	337.9	202	6913.1	197	609.0
0.515	0.063	63	600.6	104	466.0	75	282.4	276	9706.9	184	542.0
0.602	0.027	46	383.5	80	308.0	66	229.7	172	4685.2	152	409.1
0.800	0.002	24	193.6	45	133.8	32	92.2	74	1077.2	70	169.8

References

- Onureena Banerjee, Laurent El Ghaoui, and Alexandre DAspremont. Model Selection Through Sparse Maximum Likelihood Estimation for Multivariate Gaussian or Binary Data. *JMLR*, 9:485–516, 2008.
- Onkar Anant Dalal and Bala Rajaratnam. G-ama: Sparse gaussian graphical model estimation via alternating minimization. *arXiv preprint arXiv:1405.3034*, 2014.
- Jie Peng, Pei Wang, Nengfeng Zhou, and Ji Zhu. Partial Correlation Estimation by Joint Sparse Regression Models. *Journal of the American Statistical Association*, 104(486):735–746, June 2009.
- Guilherme V Rocha, Peng Zhao, and Bin Yu. A path following algorithm for Sparse Pseudo-Likelihood Inverse Covariance Estimation (SPLICE). Technical Report 60628102, 2008.
- Jerome Friedman, Trevor Hastie, and Robert Tibshirani. Applications of the lasso and grouped lasso to the estimation of sparse graphical models. Technical report, 2010.
- Kshitij Khare, Sang-Yun Oh, and Bala Rajaratnam. A convex pseudo-likelihood framework for high dimensional partial correlation estimation with convergence guarantees. *to appear in Journal of the Royal Statistical Society: Series B*, 2014.
- Amir Beck and Marc Teboulle. A fast iterative shrinkage-thresholding algorithm for linear inverse problems. *SIAM Journal on Imaging Sciences*, 2(1):183–202, 2009.
- R.T. Rockafellar. Monotone operators and the proximal point algorithm. *SIAM Journal on Control and Optimization*, 14(5):877–898, 1976.
- Yurii Nesterov. A method of solving a convex programming problem with convergence rate $\mathcal{O}(1/k^2)$. In *Soviet Mathematics Doklady*, volume 27, pages 372–376, 1983.
- J. Barzilai and J.M. Borwein. Two-point step size gradient methods. *IMA Journal of Numerical Analysis*, 8(1): 141–148, 1988.
- Gaël Guennebaud, Benoît Jacob, et al. Eigen v3. <http://eigen.tuxfamily.org>, 2010.
- Howard Y Chang, Dimitry S A Nuyten, Julie B Sneddon, Trevor Hastie, Robert Tibshirani, Therese Sørbye, Hongyue Dai, Yudong D He, Laura J van’t Veer, Harry Bartelink, Matt van de Rijn, Patrick O Brown, and Marc J van de Vijver. Robustness, scalability, and integration of a wound-response gene expression signature in predicting breast cancer survival. *Proceedings of the National Academy of Sciences of the United States of America*, 102(10):3738–43, March 2005.

Supplementary Materials

A Timing comparison

A.1 Median Speed-up

Table 4: Median speed-up ratio over CONCORD method and (standard deviation).

p	n	Relative to concord	
		ccista_0	ccfista_1
1000	250	0.6 (0.7)	0.4 (0.3)
1000	750	3.4 (1.8)	1.9 (0.9)
1000	1250	23.1 (5.7)	12.0 (3.5)
3000	750	2.7 (2.1)	1.9 (1.6)
3000	2250	12.8 (1.6)	8.8 (2.2)
3000	3750	81.9 (6.6)	58.2 (8.7)
5000	1250	5.6 (3.2)	3.0 (1.8)
5000	3750	21.1 (2.6)	13.5 (2.6)
5000	6250	145.8 (6.6)	110.1 (16.4)

A.2 Comparison among CONCORD-ISTA and CONCORD-FISTA variations

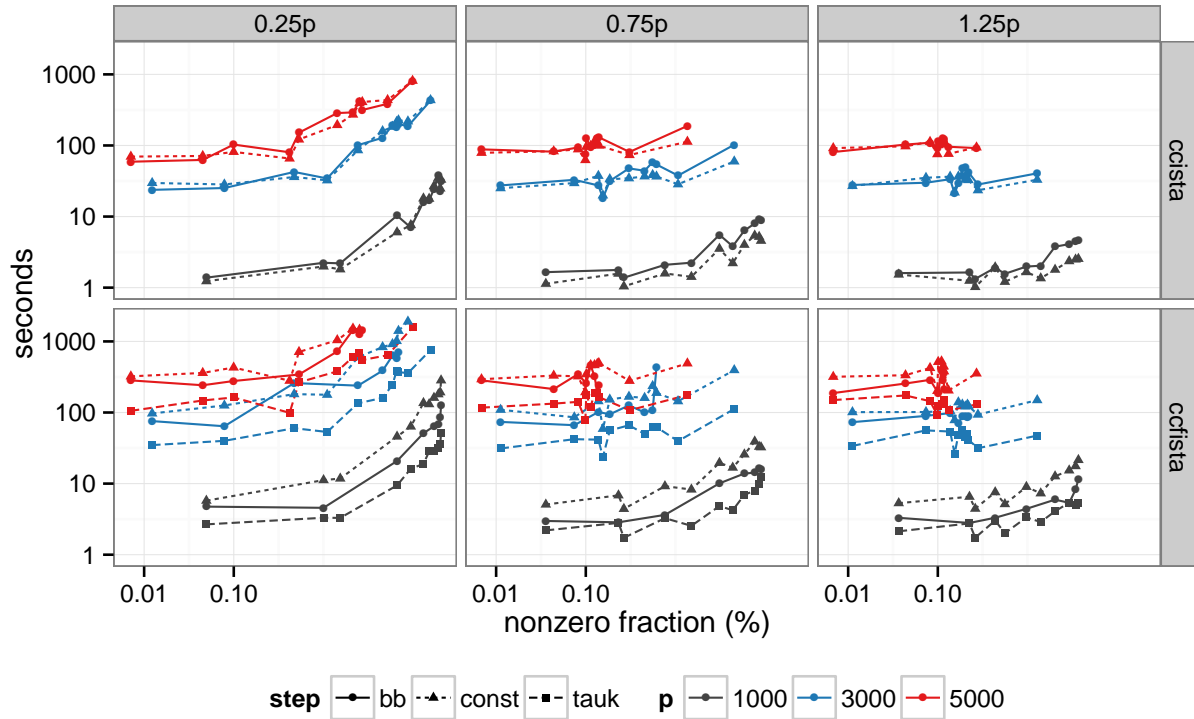


Figure 2: Timings of CONCORD-ISTA (top) and CONCORD-FISTA (bottom) variations for sample sizes $n = \{0.25p, 0.75p, 1.25p\}$

A.3 Comparison with CONCORD algorithm

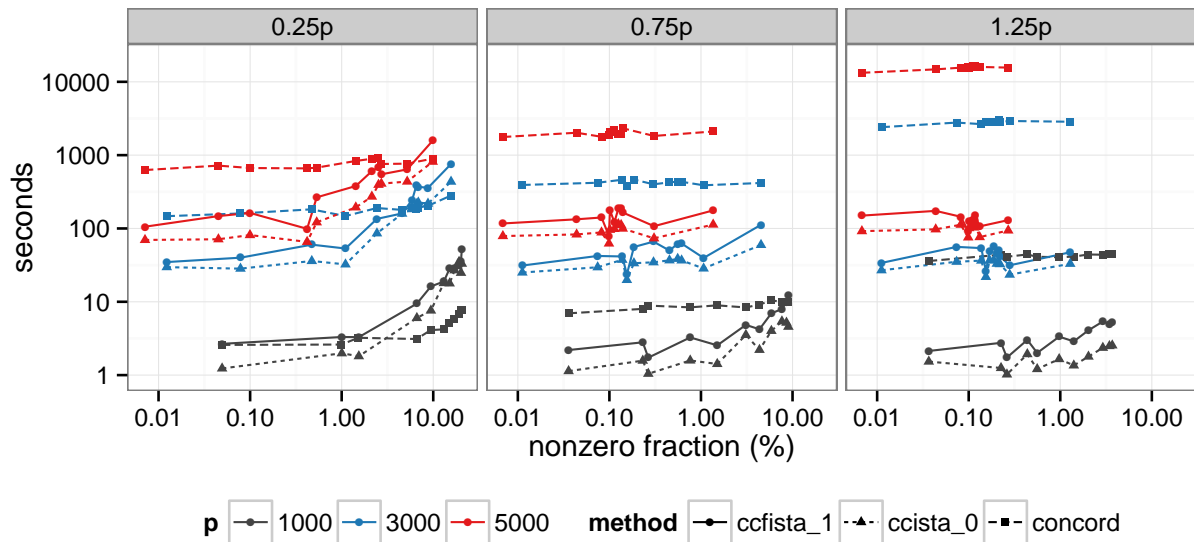


Figure 3: Timing of best CONCORD-ISTA and CONCORD-FISTA variations against CONCORD for sample sizes $n = \{0.25p, 0.75p, 1.25p\}$.

A.4 Running times

Table 5: $p = 1000$, true non-zero fraction (nzf) of 1%

	p	n	λ	nzf (%)	concord		ccista_0		ccfista_1	
					iter	seconds	iter	seconds	iter	seconds
7	1000	250	0.163	0.99	9	2.61	18	1.98	26	3.31
8	1000	250	0.300	0.05	9	2.58	15	1.23	23	2.67
9	1000	750	0.058	8.99	10	9.96	20	4.56	28	12.44
10	1000	750	0.059	8.56	10	9.86	20	5.19	28	9.86
11	1000	750	0.061	7.64	10	9.97	20	5.41	28	7.96
12	1000	750	0.066	5.86	10	10.45	20	4.01	27	6.96
13	1000	750	0.077	3.09	9	8.37	16	3.53	25	4.84
14	1000	750	0.103	0.76	9	8.40	15	1.58	24	3.26
15	1000	750	0.163	0.23	9	8.00	15	1.57	24	2.80
16	1000	750	0.300	0.04	8	6.96	13	1.13	18	2.20
17	1000	1250	0.058	3.69	9	44.21	15	2.54	24	5.29
18	1000	1250	0.059	3.43	9	44.25	16	2.49	24	5.00
19	1000	1250	0.061	2.91	9	43.84	16	2.36	24	5.38
20	1000	1250	0.066	2.03	9	44.15	14	1.79	24	4.09
21	1000	1250	0.077	0.97	9	40.50	15	1.65	24	3.34
22	1000	1250	0.103	0.44	9	44.16	15	1.93	24	3.02
23	1000	1250	0.163	0.23	9	43.84	13	1.25	23	2.75
24	1000	1250	0.300	0.04	8	35.99	13	1.53	17	2.13

Table 6: $p = 3000$, true non-zero fraction (nzf) of 0.33%

	p	n	λ	nzf (%)	concord		ccista_0		ccfista_1	
					iter	seconds	iter	seconds	iter	seconds
29	3000	750	0.077	2.42	18	190.00	36	85.81	31	135.13
30	3000	750	0.103	0.47	17	182.36	28	36.00	35	60.13
31	3000	750	0.163	0.08	16	160.13	28	28.29	26	39.94
32	3000	750	0.300	0.01	15	147.07	25	29.67	23	34.80
33	3000	2250	0.058	0.61	16	433.05	27	36.63	26	62.26
34	3000	2250	0.059	0.56	16	434.96	28	38.50	26	61.90
35	3000	2250	0.061	0.45	16	425.58	28	36.75	26	50.02
36	3000	2250	0.066	0.30	16	400.08	28	34.55	34	66.10
37	3000	2250	0.077	0.19	16	464.53	28	33.57	32	55.90
38	3000	2250	0.103	0.14	16	462.08	28	37.39	24	41.50
39	3000	2250	0.163	0.07	15	420.28	26	29.57	25	42.17
40	3000	2250	0.300	0.01	14	391.94	22	25.06	22	31.20
41	3000	3750	0.058	0.22	16	2837.71	27	32.61	24	41.36
42	3000	3750	0.059	0.21	16	2993.98	27	33.59	24	50.58
43	3000	3750	0.061	0.20	16	2826.17	27	33.06	24	45.75
44	3000	3750	0.066	0.19	16	2805.85	27	36.94	31	57.06
45	3000	3750	0.077	0.17	15	2792.55	26	36.61	31	48.96
46	3000	3750	0.103	0.14	15	2649.75	26	36.43	31	53.95
47	3000	3750	0.163	0.07	15	2780.53	25	35.12	32	56.06
48	3000	3750	0.300	0.01	13	2406.49	22	26.91	22	33.90

Table 7: $p = 5000$, true non-zero fraction (nzf) of 0.20%

	p	n	λ	nzf (%)	concord		ccista_0		ccfista_1	
					iter	seconds	iter	seconds	iter	seconds
49	5000	1250	0.058	2.71	18	757.67	38	408.49	40	547.93
50	5000	1250	0.059	2.52	18	903.05	37	393.77	40	681.49
51	5000	1250	0.061	2.13	18	892.30	36	272.03	40	604.35
52	5000	1250	0.066	1.42	17	832.68	32	193.88	37	379.23
53	5000	1250	0.077	0.53	17	674.71	30	121.39	35	265.84
54	5000	1250	0.103	0.10	17	667.62	27	81.21	33	163.00
55	5000	1250	0.163	0.05	16	719.81	25	71.23	34	147.53
56	5000	1250	0.300	0.01	14	626.20	25	69.71	30	105.65
57	5000	3750	0.058	0.14	17	2324.54	29	99.50	35	165.12
58	5000	3750	0.059	0.13	17	1965.36	29	111.53	35	189.05
59	5000	3750	0.061	0.13	17	1967.39	29	114.72	35	186.34
60	5000	3750	0.066	0.11	17	2183.90	29	98.54	25	121.39
61	5000	3750	0.077	0.10	17	2094.73	29	95.84	33	178.13
62	5000	3750	0.103	0.08	16	1780.97	26	88.29	32	141.14
63	5000	3750	0.163	0.04	16	2021.49	25	82.88	33	133.36
64	5000	3750	0.300	0.01	14	1767.63	24	78.77	30	117.03
65	5000	6250	0.058	0.12	17	15698.02	27	113.65	25	150.95
66	5000	6250	0.059	0.12	17	16221.44	27	115.35	25	130.19
67	5000	6250	0.061	0.11	17	15698.53	27	103.06	25	132.57
68	5000	6250	0.066	0.11	17	16220.33	27	111.75	25	129.70
69	5000	6250	0.077	0.10	17	15671.14	27	101.03	25	123.92
70	5000	6250	0.103	0.08	17	15600.83	26	112.48	33	144.42
71	5000	6250	0.163	0.04	16	14787.78	26	97.33	34	173.66
72	5000	6250	0.300	0.01	14	13287.76	24	91.84	30	149.70

A.5 Other Methods

A.5.1 Dual problem of CONCORD

Formulating the dual using the matrix form is challenging since the KKT conditions involving the gradient term $S\Omega + \Omega S$ do not have a closed form solution as in the case of Gaussian problem in Dalal and Rajaratnam [2014]. Therefore, we consider a vector form of the CONCORD problem by defining two new variables $x_1 \in \mathbb{R}^p$ and $x_2 \in \mathbb{R}^{p(p-1)/2}$ as

$$\begin{aligned} x_1 &= (\omega_{11}, \omega_{22}, \dots, \omega_{pp})^T \\ x_2 &= (\omega_{12}, \omega_{13}, \dots, \omega_{1p}, \omega_{23}, \dots, \omega_{2p}, \dots, \omega_{p-1p})^T. \end{aligned} \quad (21)$$

We define two coefficient matrices A_1, A_2 as

$$A_1 = \begin{bmatrix} Y_1 & & & & \\ & Y_2 & & & \\ & & \ddots & & \\ & & & Y_p & \end{bmatrix}, A_2 = \begin{bmatrix} Y_2 & Y_3 & \cdots & Y_p & & & & & \\ Y_1 & & & & Y_3 & \cdots & Y_p & & & \\ & Y_1 & & & Y_2 & & & & & \\ & & \ddots & & & \ddots & & & & \\ & & & Y_1 & & & & & & \\ & & & & Y_2 & & & & & \\ & & & & & \ddots & & & & \\ & & & & & & Y_{p-1} & Y_p & & \\ & & & & & & Y_{p-2} & & Y_p & \\ & & & & & & & Y_{p-2} & Y_{p-1} & Y_p \end{bmatrix}, \quad (22)$$

where A_1 is $n \times p$ and A_2 is $n \times p(p-1)/2$ dimensional matrices. Using these definitions, the CONCORD problem (4) can be rewritten as

$$\underset{x_1, x_2}{\text{minimize}} \quad -n \log x_1 + \frac{1}{2} \|A_1 x_1 + A_2 x_2\|^2 + \lambda \|x_2\|_1. \quad (23)$$

where, $\log(x_1) = \sum_{i=1}^p \log(x_{1i})$. We will use $x = \begin{bmatrix} x_1 \\ x_2 \end{bmatrix}$ for simplicity of notation where ever possible.

The transformed CONCORD problem in (23) can be written in composite form using a new variable $z = A_1 x_1 + A_2 x_2$ as

$$\begin{aligned} \underset{x_1, x_2, z}{\text{minimize}} \quad & -n \log x_1 + \frac{1}{2} \|z\|^2 + \lambda \|x_2\|_1 \\ \text{subject to} \quad & A_1 x_1 + A_2 x_2 = z \end{aligned} \quad (24)$$

The Lagrangian for this problem is given by

$$\mathcal{L}(x_1, x_2, z, y) = -n \log x_1 + \frac{1}{2} \|z\|^2 + \lambda \|x_2\|_1 + y^T (A_1 x_1 + A_2 x_2 - z). \quad (25)$$

Maximizing with respect to the three primal variables yields following optimality conditions (the \cdot notation is adapted from MATLAB to denote element-wise operations),

$$\begin{aligned} z - y &= 0 \\ -n./x_1 + A_1^T y &= 0 \\ \lambda \text{sign}(x_2) + A_2^T y &\ni 0. \end{aligned} \quad (26)$$

Substituting these the dual problem can be written as

$$\begin{aligned} \underset{y}{\text{maximize}} \quad & -n \log n./A_1^T y + \frac{1}{2} \|y\|^2 + y^T (A_1(n./A_1^T y) - y) \\ \text{subject to} \quad & \|A_2^T y\|_\infty \leq \lambda, \end{aligned}$$

or equivalently

$$\begin{aligned} \underset{y}{\text{maximize}} \quad & \frac{1}{2} \|y\|^2 - n \log (A_1^T y) + c \\ \text{subject to} \quad & \|A_2^T y\|_\infty \leq \lambda, \end{aligned} \quad (27)$$

where, $c = n \log n - n^2$ is a constant. This problem can also be written in composite form as

$$\begin{aligned} & \underset{y}{\text{maximize}} \quad \frac{1}{2} \|y\|^2 - n \log(A_1^T y) + \mathbb{1}_{\|w\|_\infty \leq \lambda} \\ & \text{subject to} \quad A_2^T y - w = 0. \end{aligned} \quad (28)$$

The gradient and hessian of the smooth function $h(y) = \frac{1}{2} \|y\|^2 - n \log(A_1^T y)$ is given by

$$\begin{aligned} \nabla h(y) &= y - A_1(n./A_1^T y), \\ \nabla^2 h(y) &= I + A_1 \text{diag}(n./A_1^T y) A_1^T. \end{aligned} \quad (29)$$

Here, the hessian is bounded away from the semi-definite boundary. Hence the function h is strongly convex with parameter 1. Moreover, on lines of Theorem 3.1, we can show that if y is restricted to a convex level set $\mathcal{C} = \{y | h(y) \leq M\}$ for some constant M , then the function h has a Lipschitz continuous gradient. Note that

$$\begin{aligned} -n \log(A_1^T y) &\leq h(y) \leq M \\ e^{-\frac{M}{n}} &\leq A_1^T y. \end{aligned} \quad (30)$$

Therefore, the hessian satisfies

$$\nabla^2 h(y) = I + A_1 \text{diag}(n./A_1^T y) A_1^T \preceq (1 + n\rho(A_1^T A_1) e^{\frac{2M}{n}}) I. \quad (31)$$

To conclude, the dual problem provides an alternate method to prove the $\mathcal{O}(\frac{1}{k})$ and $\mathcal{O}(\frac{1}{k^2})$ rates of convergence for CONCORD problem.

A.5.2 Proximal Newton's Algorithm for CONCORD

Recall that the hessian of the smooth function h_1 as given in 6 is

$$\nabla^2 h_1(\Omega) = \sum_{i=1}^{i=p} \omega_{ii}^{-2} [e_i e_i^T \otimes e_i e_i^T] + \frac{1}{2} (S \otimes I + I \otimes S).$$

The subproblem solved for the direction of descent for the second order PNOPT algorithm is given by

$$\Delta\Omega^{(k)} = \arg \min_W \langle G^{(k)}, W \rangle + \frac{1}{2} \sum_{i=1}^{i=p} \omega_{ii}^{-2} \text{tr}(W e_i e_i^T W e_i e_i^T) + \text{tr}(WSW) + \lambda \|\Omega_X^{(k)}\| + W\|_1. \quad (32)$$

Using these, the matrix version of the second order algorithm is given in Algorithm 3. Here, the subproblem for the descent step is as a huge Lasso problem. This can be solved by standard Lasso packages which uses coordinate descent methods.

Algorithm 3 CONCORD - Proximal Newton Optimization Matrix form (CONCORD-PNOPT)

Initialize: $\Omega^{(0)} \in \mathbb{S}_+^p$, $\tau_{(0,0)} = 1$, $\Delta_{\text{opt}} = 2\epsilon_{\text{opt}}$ and $\Delta_{\text{term}} = 2\epsilon_{\text{term}}$

while $\Delta_{\text{subg}} > \epsilon_{\text{subg}}$ **or** $\Delta_{\text{term}} > \epsilon_{\text{term}}$ **do**

 Compute ∇h_1 :

$$G^{(k)} = \Omega_D^{-1} + \frac{1}{2} (S \Omega^{(k)T} + \Omega^{(k)} S)$$

 Compute Newton step:

$$\Delta\Omega^{(k)} = \arg \min_W \langle G^{(k)}, W \rangle + \frac{1}{2} \sum_{i=1}^{i=p} \omega_{ii}^{-2} \text{tr}(W e_i e_i^T W e_i e_i^T) + \text{tr}(WSW) + \lambda \|\Omega_X^{(k)}\| + W\|_1$$

 Compute sufficient descent $\Delta^{(k)}$:

$$\Delta^{(k)} = \langle G^{(k)}, \Delta\Omega^{(k)} \rangle + \lambda (\|\Omega_X^{(k)} + \Delta\Omega_X^{(k)}\|_1 - \|\Omega_X^{(k)}\|_1)$$

 Compute τ_k , such that $Q_{\text{con}}(\Omega^{(k+1)}) \leq Q_{\text{con}}(\Omega^{(k)}) + \alpha \tau_k \Delta^{(k)}$.

 Update: $\Omega^{(k+1)} = \Omega^{(k)} + \tau_k \Delta\Omega^{(k)}$

 Compute convergence criteria:

$$\Delta_{\text{subg}} = \frac{\|\nabla h(\Omega^{(k)}) + \partial g(\Omega^{(k)})\|}{\|\Omega^{(k)}\|}, \quad \Delta_{\text{term}} = \frac{\|f(\Omega^{(k+1)}) - f(\Omega^{(k)})\|}{\|f(\Omega^{(k)})\|}$$

end while
